Electric moments in molecule interferometry

2011 New J. Phys. 13 043033

(http://iopscience.iop.org/1367-2630/13/4/043033)

New Journal of Physics
The open-access journal for physics

Electric moments in molecule interferometry

Sandra Eibenberger[1], Stefan Gerlich[1], Markus Arndt[1,4], Jens Tüxen[2] and Marcel Mayor[2,3,4]

[1] University of Vienna, Vienna Center for Quantum Science and Technology (VCQ), Faculty of Physics, Boltzmanngasse 5, 1090 Vienna, Austria
[2] Department of Chemistry, University of Basel, St Johannsring 19, CH-4056 Basel, Switzerland
[3] Karlsruhe Institute of Technology, Institute for Nanotechnology, PO Box 3640, 76021 Karlsruhe, Germany
E-mail: Markus.Arndt@univie.ac.at and Marcel.Mayor@unibas.ch

New Journal of Physics **13** (2011) 043033 (11pp)
Received 16 February 2011
Published 26 April 2011
Online at http://www.njp.org/
doi:10.1088/1367-2630/13/4/043033

Abstract. We investigate the influence of different electric moments on the shift and dephasing of molecules in a matter wave interferometer. Firstly, we provide a quantitative comparison of two molecules that are non-polar yet *polarizable* in their thermal ground state and that differ in their stiffness and *response to thermal excitations*. While $C_{25}H_{20}$ is rather rigid, its larger derivative $C_{49}H_{16}F_{52}$ is additionally equipped with floppy side chains and vibrationally activated dipole moment variations. Secondly, we elucidate the role of a *permanent electric dipole moment* by contrasting the quantum interference pattern of a (nearly) non-polar and a polar porphyrin derivative. We find that a high molecular polarizability and even sizeable dipole moment fluctuations are still well compatible with high-contrast quantum interference fringes. The presence of permanent electric dipole moments, however, can lead to a dephasing and rapid degradation of the quantum fringe pattern already at moderate electric fields. This finding is of high relevance for coherence experiments with large organic molecules, which are generally equipped with strong electric moments.

[4] Authors to whom any correspondence should be addressed.

Contents

1. From polarizability to permanent moments in Kapitza–Dirac–Talbot–Lau interferometry

Molecule interferometry builds on successful research in matter wave coherence with elementary and atomic particles [1]–[4], and extends this field by the internal complexity of large many-body systems that may be thermally highly excited. Over the last few years, molecule interferometry has also developed into a tool for quantitative metrology: de Broglie interference is, per definition, associated with the particle's center of mass [5], but recent experiments have shown that the internal states of delocalized objects may play an important role in the visibility and phase shift of interference fringes. This has been exploited to measure the optical α_{opt} [6] or static polarizability α_{stat} [7] of molecules. Diffraction was used to identify the mass of weakly bound He dimers [8] and in hydrogen clusters [9]. The combination of near-field quantum fringes with classical Stark deflectometry [10] allows one to also distinguish structural isomers [11] and to sort molecular beams according to intramolecular properties [12]. The same method is interesting for identifying the onset of thermal fragmentation [13], measuring absolute single-photon absorption cross sections [14] and revealing the presence of thermally induced dipoles in vibrating molecules [15].

Our present work now contrasts three possible molecular responses to an inhomogeneous electric field in a matter wave interferometer. We study their polarizabilities, the presence of *fluctuating* dipoles and, for the first time, the effect of a *permanent* but randomly oriented electric dipole moment. The separation of the effects becomes possible by a pairwise comparison within a set of four molecules. For simplicity we will designate them as compounds (1)–(4). Their shapes and sum formulae are given in figure 1. Compounds (1) and (2) are tetraphenylmethane derivatives that were tailor-made and purified in our labs in Basel for the particular purpose of these coherence experiments. The porphyrin derivatives (3) and (4) were purchased from Porphyrin Systems and used without further purification. We use electric deflectometry inside a Kapitza–Dirac–Talbot–Lau interferometer (KDTLI) [16], as sketched in figure 2, and study the influence of the internal properties on the persistence of quantum coherence. The overall idea is a quantum extension of classical beam methods that have already been successfully applied to characterize clusters [17]–[20] and molecules [21, 22] or even to sort such particles according to their internal configuration [23].

In our new experiments the comparison of tetraphenylmethane $C_{25}H_{20}$ (1) with its larger brother $C_{49}H_{16}F_{52}$ (2) allows us first to locate the structural origin of fluctuating dipole moments in these compounds. Our subsequent analysis of iron-loaded tetraphenylporphyrin (3) and its

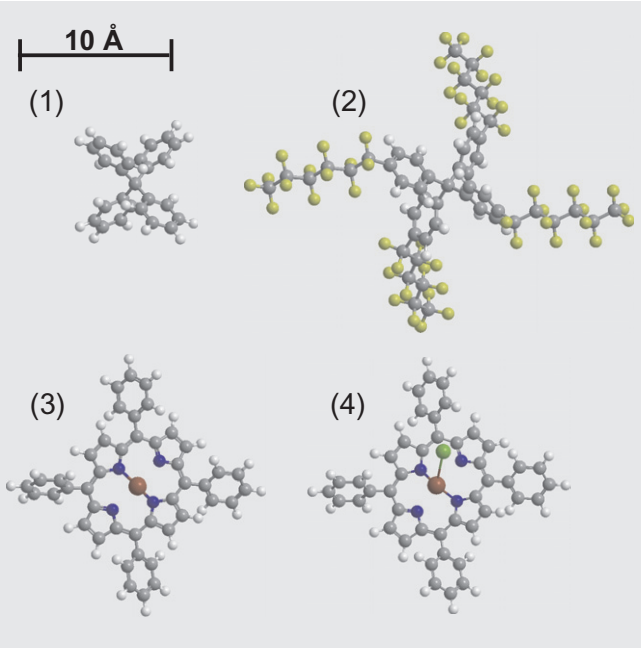

Figure 1. Gallery of molecules used in our present KDTL–Stark deflectometry experiments. (1) A rigid, non-polar molecule: tetraphenylmethane $C_{25}H_{20}$, $m = 320$ amu. (2) A floppy molecule with thermal dipole fluctuations: perfluoroalkylated tetraphenylmethane $C_{49}H_{16}F_{52}$, $m = 1592$ amu. (3) The (nearly) non-polar FeTPP: $C_{44}H_{28}FeN_4$, $m = 668$ amu. (4) The polar FeTPPCl: $C_{44}H_{28}ClFeN_4$, $m = 704$ amu. It differs from (3) by the addition of a single chlorine atom.

chlorine-extended partner (4) then illustrates the detrimental effect of permanent dipoles on the interference contrast in the presence of external field inhomogeneities.

A molecular beam is formed by sublimating from a pure powder. The particles travel about 2.5 m through ultrahigh vacuum before they are detected using electron impact ionization quadrupole mass spectrometry. We use a free-fall trajectory selection scheme [24] to filter out a longitudinal velocity band. The interferometer is composed of three gratings [25]. The first SiN grating, G_1, with a period of $d = 266$ nm, serves to select a molecular ensemble of sufficient transverse coherence such that each de Broglie wave can be regarded as being delocalized over the width of a few slits. The second grating, G_2, is an intense standing light wave ($P < 18$ W) along the z-direction with a waist of $w_x = 20\,\mu$m and a height of about 1 mm, varying between the different experiments. The oscillating electric light field represents a diffracting phase mask for the incident matter waves, with $\Phi(x) \propto \alpha_{\rm opt} P \sin^2(kz)$, where $\alpha_{\rm opt}$ is the molecular optical polarizability at the laser wavelength. When a delocalized molecule encounters simultaneously at least two neighboring antinodes of G_2, the situation resembles locally a double-slit experiment where the particle can travel along two paths from the source to the detector. The different probability amplitudes along all paths add up to generate a periodic molecular density pattern at the location of the third grating G_3. The resulting interference fringes are imaged by scanning G_3 across the beam while recording the transmitted molecules.

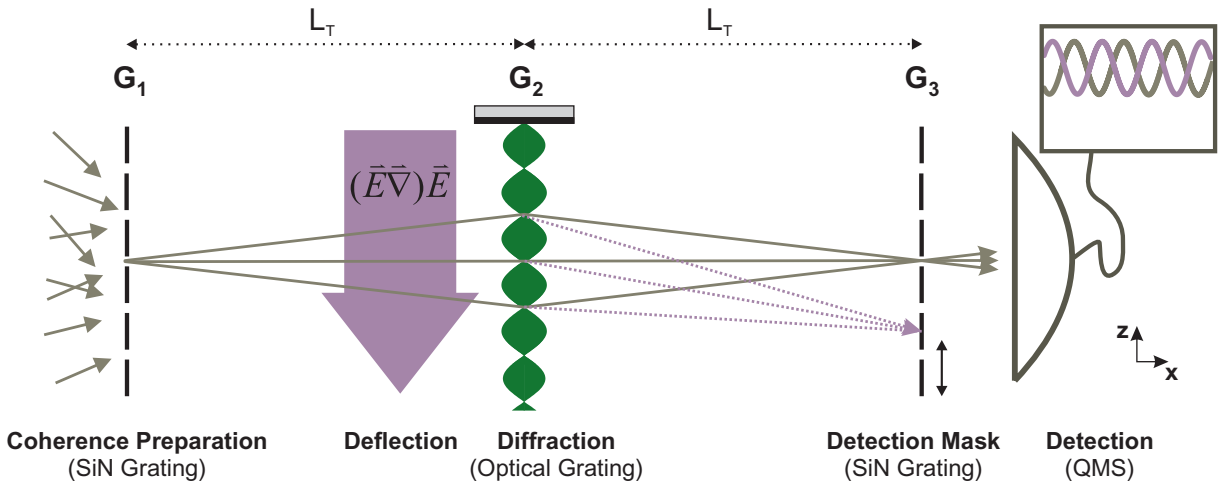

Figure 2. The KDTL metrology experiment allows one to combine matter wave interferometry with Stark deflectometry to study the internal electric properties of complex molecules. The molecular polarizability α_{stat} and thermally fluctuating dipole moments contribute to the susceptibility χ and to the shift of the interference pattern in the external electric field, independent of the molecular orientation. A permanent electric dipole moment interacts with the same field but the fringe shift now depends on the molecular alignment with the field.

2. Locating weak links in a delocalized molecule

Earlier work [15, 26] already showed that thermally excited flexible molecules may exhibit vibrationally induced electric dipole moments. Here we go one step further and compare the relative rigidity of *substructures inside* the delocalized molecules. The overall idea of the experiments is as follows: two molecular species are tailored to share an identical core. However, compound (2) is enlarged with respect to (1) by the addition of four perfluoroalkyl chains. For both compounds the *static polarizability* can be computed and compared to the interferometric measurement. The numerical results compare rather well with our findings for the *optical polarizability* of compound (2), which is a good approximation to α_{stat} if the probing laser wavelength lies outside any molecular resonance. For both compounds, we also measure the *electric susceptibilities* [10] that include the presence of possible dynamical dipole moments [26]. For compound (1) this value compares favorably with the computed polarizability, whereas it is in marked discrepancy for molecule (2). This allows us to identify the vibrationally activated dipoles in the side arms of compound (2) as the origin of its observed susceptibility increase.

The first molecule (1) was synthesized by an electrophilic aromatic substitution of trityl-chloride and aniline, and subsequent deamination [27]. Its perfluoroalkylated counterpart (2) was assembled in two steps starting from tetraphenylmethane. Terminal functionalization of all four phenyl rings was achieved by bromination [28] and a subsequent coupling of the four fluorous ponytails in an Ullmann-type reaction [11]. Both compounds (1) and (2) were characterized by NMR spectroscopy, elemental analysis and mass spectrometry.

A numerical model using MM2 force field calculations [29] of both molecules at $T = 480\,\mathrm{K}$ reveals the rigid character of (1) and the high flexibility of (2), which is caused by

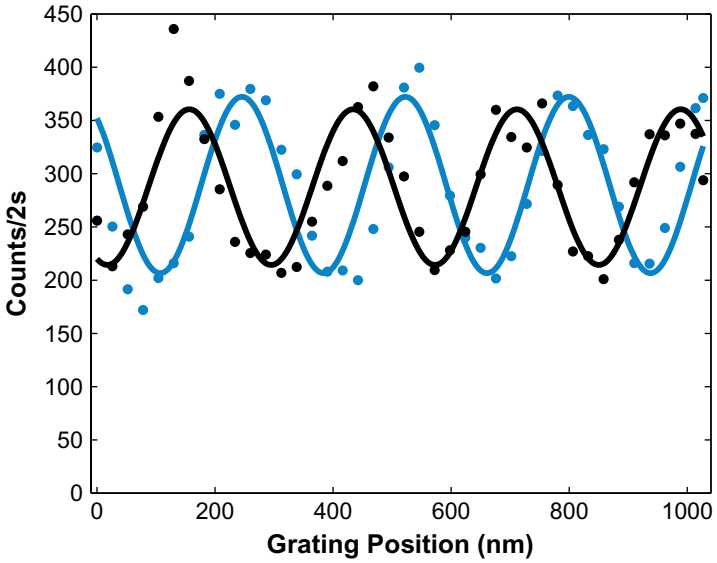

Figure 3. The quantum interference pattern is shifted when a homogeneous electric force field acts transversally on the delocalized molecules. Induced dipoles interact only in second order with the field: the force therefore maintains its sign even when the field is reversed or when the molecular orientation is rotated. Permanent electric dipole moments interact already in first order with the field. Different molecular orientations therefore lead to different phase shifts. Here: shift of the non-polar compound (2) at a deflection voltage of 5 kV (blue dots) compared with the interference pattern at a reference voltage of 1 kV (black dots) applied to the electrodes. The measured dark rate is already subtracted and the solid lines represent sinusoidal fits to the data.

the attached side chains. This intramolecular feature can be revealed experimentally by adding a pair of electrodes, in between the first and second gratings, which is designed to provide a force field $\mathbf{F} \propto \chi(\mathbf{E}\nabla)\mathbf{E}/mv^2 \propto \hat{\mathbf{z}}$, which is homogeneous to within 1% across the entire molecular beam [30]. The force acts on the electric susceptibility $\chi = \alpha_{\rm stat} + \langle d_z^2\rangle/3k_{\rm B}T$ [31], which comprises both the electronic contribution $\alpha_{\rm stat}$ and a part related to the thermally averaged squared projection of the electric dipole moment onto the electric field axis $\langle d_z^2\rangle$.

The two tailor-made molecular compounds (1) and (2) differ by their structural rigidity, which influences their electric properties. Using the simulation package Gaussian09 [32] with the basis set 6–31G*, we compute the *static* polarizabilities to be $\alpha_{\rm stat}(1) = 4\pi\varepsilon_0 \times 33\,\text{Å}^3$ and $\alpha_{\rm stat}(2) = 4\pi\varepsilon_0 \times 69\,\text{Å}^3$. For far-off resonant laser light, the static value is a good approximation to the optical polarizability, $\alpha_{\rm opt}(1, 2)$, and we have verified that it depends only within a few percent on the particular configuration of the molecules.

The *optical* polarizability can experimentally be extracted from the dependence of the interference contrast on the laser power in G_2 [6]. Our experiment for compound (2) finds $\alpha_{\rm opt}(2) = 4\pi\varepsilon_0 \times 71(4)\,\text{Å}^3$, in good agreement with the computed static value. The properties of the freely propagating molecules are thus well characterized.

We now expose the molecular beam to the external electric force and observe a fringe shift that increases quadratically with the applied voltage. To give an example, the shift of the interference pattern of compound (2) is shown in figure 3 for a deflection voltage of 5 kV.

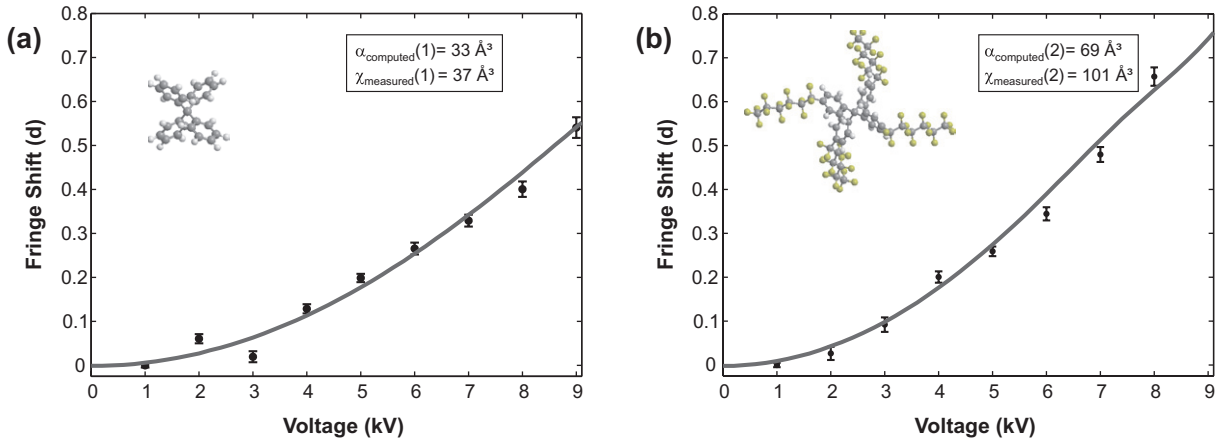

Figure 4. KDTLI-deflection experiments with compounds (1) and (2). (a) Fringe shift of (1) measured in multiples of the grating period d as a function of deflection voltage. The mean velocity is $v(1) = 220\,\mathrm{m\,s^{-1}}$ and the velocity spread is $\Delta v/v(1) = 0.22$. The computed value for the static polarizability $\alpha_{\mathrm{stat}}(1) = 4\pi\varepsilon_0 \times 33\,\mathrm{Å}^3$ is in good agreement with the experimental value for the susceptibility of $\chi(1) = 4\pi\varepsilon_0 \times 37(3)\,\mathrm{Å}^3$, which we extract from a numerical fit to the data (solid gray line). (b) Fringe deflection of compound (2), with $v(2) = 122\,\mathrm{m\,s^{-1}}$ with $\Delta v/v(2) = 0.18$. In comparison to the computed static polarizability $\alpha_{\mathrm{stat}}(2) = 4\pi\varepsilon_0 \times 69\,\mathrm{Å}^3$, the experiment shows a considerably enhanced susceptibility $\chi(2) = 4\pi\varepsilon_0 \times 101(4)\,\mathrm{Å}^3$ that can be assigned to thermally activated conformation changes and fluctuating dipole moments [15, 26].

From a fit to the shift-versus-voltage curve, we can extract the experimental susceptibility value $\chi(1) = 4\pi\varepsilon_0 \times 37(3)\,\mathrm{Å}^3$ for compound (1), which is in good agreement with the computed polarizability.

In marked contrast to that, the susceptibility of derivative (2) shows a substantially enhanced $\chi(2) = 4\pi\varepsilon_0 \times 101(4)\,\mathrm{Å}^3$. This is a strong indication of the presence of thermally activated conformation changes on a short time scale. They allow for a temporary electric dipole moment whose squared projection does not average out. For both compounds (1) and (2) the fringe deflection as a function of the applied voltage is shown in figure 4.

The deflection experiment thus supports the computed picture of a rigid tetraphenylmethane core and flexible side chains with structural weak links, that enhance the susceptibility through rapidly fluctuating dipole moments. The quantitative value of this contribution is sizeable and important with regard to future experiments, where long perfluoroalkyl side chains are used in an attempt to increase the mass limits in organic interference while maintaining the particles sufficiently weakly bound to be able to launch them in an effusive beam.

3. Orientation averaging of permanent electric dipole moments

A second conclusion of the previous section is even more important: quantum coherence can be maintained, in spite of all fluctuations and transitions between the internal molecular states, as long as this dynamics does not introduce which-path encoding or random trajectory noise. Pictorially, even though the internal configuration may change at a high rate, it does so in all

spatial positions at the same time. As long as the internal state is decoupled from the center of mass motion, a pure de Broglie interference experiment will only see the internal states through phase shifts caused in conservative interactions with the environment.

In the above example, a *polarizable* molecule will always be deflected in the same direction, independent of its own spatial orientation. The same is true to first order for a *floppy* molecule, where fluctuating dipoles will preferentially orient themselves in such a way as to mimic the effects of enhanced polarizability.

The situation changes in the presence of *permanent electric dipoles* of *rigid molecules*, which we now study in a comparison of the two porphyrin derivatives displayed in figure 1. The iron-loaded FeTPP (3) and its polar derivative FeTPPCl (4) can be easily distinguished in the quadrupole mass spectrum. The mass difference is as little as 5% and should be negligible for the effective distribution of de Broglie wavelengths, which is largely dominated by the broad velocity spread of $\Delta v/v \simeq 20\%$. The addition of a single chlorine atom establishes, however, a large permanent electric dipole moment of approximately $d = 2.7$ Debye [33][5]. The structure of iron–porphyrin has been discussed a lot in the literature. Interestingly, the position of the Fe-atom relative to the porphyrin plane depends on the nature of the bond [34] and on the molecular spin. The displacement from the N-plane has been predicted to vary from 0.24 Å for the singlet state over 0.15 Å for the triplet state to 0.33 Å for the quintet [35]. This rather small displacement is the reason why in the following we will designate the nature of FeTPP as (almost) non-polar, in comparison to FeTPPCl. This difference is also revealed in our quantum interference experiments where a static dipole moment can drastically lower the interference fringe contrast in the presence of an external field.

In figure 5 we compare the fringe visibility for both molecules as a function of diffracting laser power. Within experimental uncertainty the quantum contrast is the same, which means that the de Broglie wave spectra and also the optical polarizabilities are the same within a few percent.

The simple addition of a single chlorine atom is expected to change neither the static polarizability nor any possibly existing thermally activated dipole moment by much. A KDTL deflectometry experiment confirms this view, as long as we focus our attention on the *shift* of the interference pattern in the presence of the electric field. Figure 6 verifies that both species follow the same deflection parabola, as expected from $\Delta x \propto \chi(\mathbf{E}\nabla)\mathbf{E}/mv^2 \propto \chi U^2/m$, where the electric field $\mathbf{E}$ is proportional to the applied electric voltage U.

The situation changes drastically when we compare the fringe *visibilities* of the two derivatives (3) and (4) as a function of the applied voltage. Figure 7 shows that the quantum contrast of the chlorinated polar molecule (4) decays significantly faster than that of the non-polar compound (3). The intuitive picture behind this observation is as follows. If we expose the non-polar FeTPP (3) to the external electric field, this induces a dipole moment that is always deflected towards higher field strengths. The fringe shift grows quadratically but the visibility should remain constant as a function of the applied voltage as long as we can neglect the molecular velocity spread.

The faster decay in the $V(U)$ curve of compound (4) in figure 7 is interpreted as follows. Molecular simulations show that tetraphenylporphyrin is mechanically rather stiff. We can

[5] In this paper [33], a thermal FeTPP fragment of FeTPPCl was misinterpreted as the post-ionization fragment of an FeTPPCl molecule that was still intact in the interferometer. Instead these measurements most likely always observed FeTPP, alone. The fact that these earlier measurements inside a mechanical Talbot–Lau deflectometer showed no indication of a permanent dipole moment is fully consistent with our present results for FeTPP.

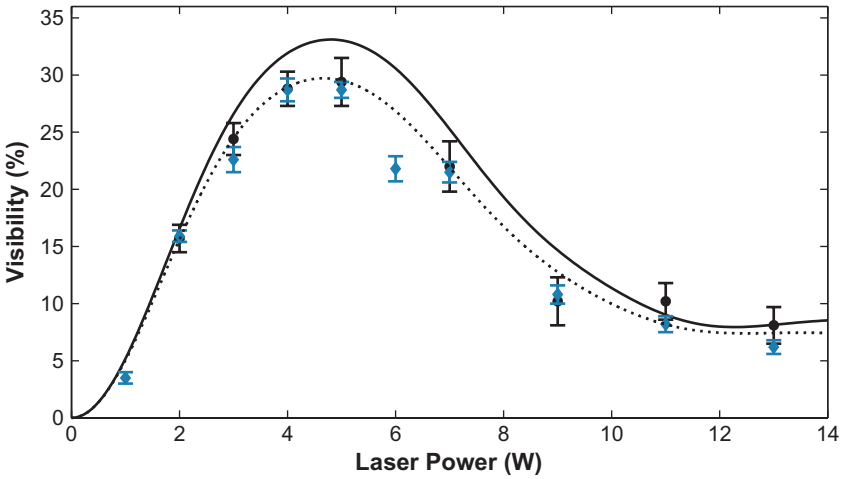

Figure 5. Fringe visibility V as a function of diffracting laser power P for the (almost) non-polar (3, black dots) and the polar (4, blue squares) porphyrin derivative. The black solid line represents the quantum fit with a polarizability of $\alpha = 4\pi\varepsilon_0 \times 108\,\text{Å}^3$; the black dashed line includes an assumed absorption coefficient of $\sigma = 5 \times 10^{-22}\,\text{m}^2$. The good agreement between both variants and the theoretical quantum expectation [6] illustrates that de Broglie interferometry does not distinguish the internal states in the absence of external fields. The molecules were sublimated at $T \approx 700\,\text{K}$ and the velocity distribution is characterized by $v(3) = 216\,\text{m s}^{-1}$ with $\Delta v/v(3) = 0.23$ and $v(4) = 207\,\text{m s}^{-1}$ with $\Delta v/v(4) = 0.24$.

therefore approximate it as an asymmetric top. The rotation around the vertical symmetry axis on the aromatic plane has a moment of inertia of $2.6 \times 10^{-43}\,\text{kg m}^2$. The sublimated molecules cover several hundred rotational quantum numbers, with a most probable $J = 475$ at $T = 700\,\text{K}$. In a classical picture the molecules are spinning rapidly, at a most probable frequency of $\nu_{\text{rot}} = 1.9 \times 10^{11}\,\text{Hz}$. The dipole moment components perpendicular to the molecular axis of rotation will average out during the transit time ($\sim 400\,\mu\text{s}$) through the deflection region. The electric force $\mathbf{F} = -\nabla(\mathbf{d}\cdot\mathbf{E})$ will correspondingly be reduced. A net effect will only persist for the dipole components parallel to the rotation axis, and in the ensemble the molecular axes are isotropically oriented with respect to the external field axis as long as the thermal energy exceeds the electric dipole interaction energy. In our experiment the thermal energy per degree of freedom is $E_{\text{therm}} = k_{\text{B}}T/2 \simeq 30\,\text{meV}$ and exceeds the electric energy of $E_{\text{el}} \leqslant -\mathbf{d}\cdot\mathbf{E} \simeq 0.1\,\text{meV}$ by more than two orders of magnitude for $d = 2.7\,\text{Debye}$ [33] and $E = 2.15 \pm 0.05 \times 10^6\,\text{V m}^{-1}$ at 5 kV applied to the electrodes. Differently oriented polar molecules will then be deflected in different directions. The isotropic orientation distribution therefore leads to an averaging over fringe shifts whose direction and strength vary with the angle between the molecular moment and the external electric field. In our present configuration, the force $F_{\mathbf{dip}} \propto (\nabla\mathbf{d})\cdot\mathbf{E}$ also varies by about 20% across our molecular beam.

The influence of the dipole moment is experimentally readily seen. In the absence of electric fields, compounds (3) and (4) have almost identical interference patterns. Both the dependence of the fringe visibility on the laser power (figure 5) and the susceptibility-dependent fringe shift (figure 6) are the same. We measure, however, a marked difference in the fringe visibility (figure 7) already when we apply an external potential of $U = 500\,V$.

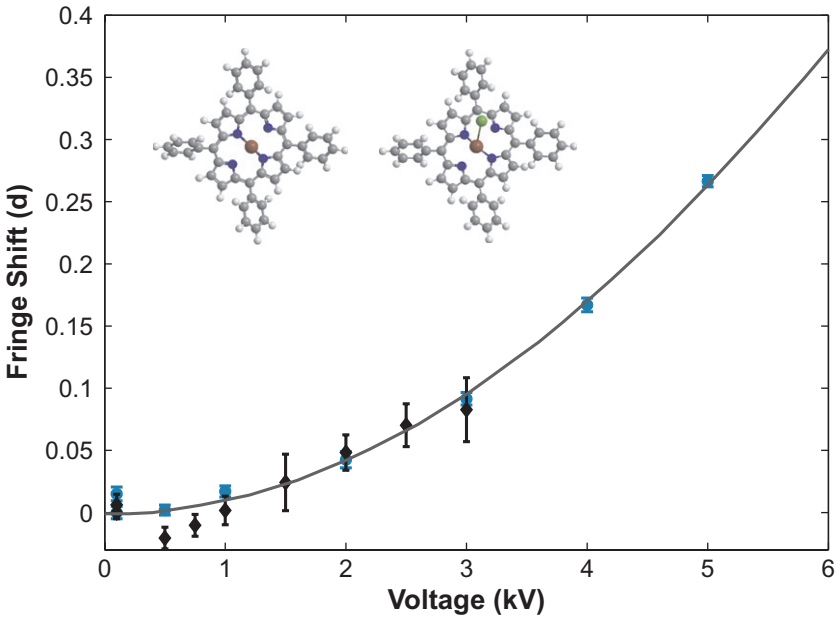

Figure 6. Fringe shift as a function of deflector voltage: both the polar (4, blue squares) and the non-polar (3, black dots) porphyrin derivatives exhibit the *same static polarizability* and therefore the same fringe deflection. The gray solid line shows the quantum fit for a static polarizability of $\alpha_{\mathrm{stat}} = 4\pi\varepsilon_0 \times 108\,\text{Å}^3$, which agrees well with earlier measurements on FeTPP [33].

Interestingly, in the first run of experiments we saw good fringe visibilities for the non-polar porphyrin (3) but never any quantum interference with the chlorinated derivative (4), even after all voltages to the deflector system had been switched off. This is consistent with the hypothesis that electric patch fields, possibly caused by tiny discharges from the electrodes towards their ceramic holders, were responsible for the observed fringe averaging. The deflector system is mounted in a vacuum of about 10^{-8} mbar and the patch charges would not disappear until after several hours. Only after insertion of a metallic end cap in both the entrance and the exit hole of the electrode holder were the interference capabilities restored for the chlorinated molecules, as well. Although it is not possible to determine the number of residual charges on the ceramic surface in hindsight and *in situ*, an estimate may motivate the high sensitivity of polar molecules to surprisingly little charge ensembles: the acceleration of a dipole moment $d = 10^{-29}\,\text{C m}$ in the presence of a single (!) electron at a distance $r = 100\,\mu\text{m}$ is $a = -\nabla(d \cdot E)/m = -de/2m\pi\varepsilon_0 r^3 = 0.02\,\text{m s}^{-2}$. Accordingly, small electron patches isolated at the rim of the ceramic collimator can already exert a force that is sufficient to shift the quantum fringe by one grating period. Since many charges may be statistically distributed on the hole surface, the net effect is efficient phase averaging over all partial interferograms of the isotropically oriented molecular ensemble.

4. Conclusion

Summarizing, we have shown that quantum interferometry with tailored and delocalized molecules allows us to assign the rigid and the floppy components inside a molecule. We

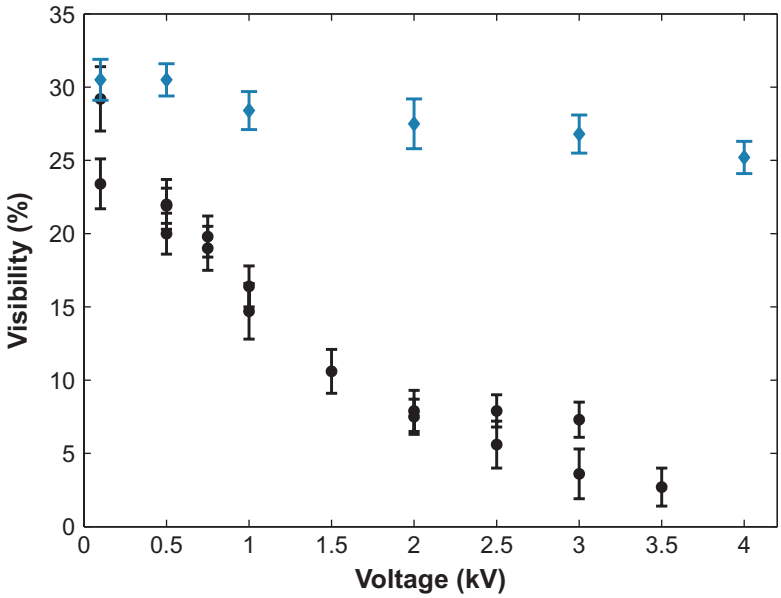

Figure 7. Quantum contrast as a function of deflection voltage. The (nearly) non-polar FeTTP (blue squares) is slightly dephased because of the finite velocity spread in the molecular beam: different particles traverse the Stark deflector for different interaction times and larger voltages enhance the different shifts between separate velocity classes. The polar FeTPPCl (black dots) is highly sensitive to the external field as differently oriented molecules will also be deflected in different directions by different amounts.

could discern the threefold possible response of neutral molecules to an external electric field. The interference pattern of a complex but non-polar and rigid molecule (1, $m = 320$ amu) is shifted to the region of higher field strength. Additional structural flexibility in a five times more massive derivative (2, $m = 1592$ amu) contributes a vibrationally induced term to the electric susceptibility that enhances the fringe shift similar to an increased polarizability. In both cases the fringe contrast is only slightly reduced at high field strengths. In variance to that, the presence of a static dipole moment may already cause dramatic fringe averaging, as demonstrated in the comparison of (3) and (4). And even small charge patches in the vicinity of the molecular beam can destroy the interference pattern completely.

A good quantitative understanding of the relative influence of all three contributions is important for the design of new quantum experiments that aim at the observation of coherence with even larger organic molecules. A vast majority of naturally occurring organic particles is equipped with a sizeable dipole moment and thus prone to dephasing in stray electric fields. One counter-strategy is to synthesize tailor-made complexes that allow us to increase the mass and size limit while maintaining the high volatility and the non-polar character of the components.

Acknowledgments

We gratefully acknowledge support from the ESF EuroQuasar program MIME, the FWF programs Wittgenstein (Z149-N16) and CoQuS (W1210-2), the DFG Centre for Functional Nanostructures (CFN) and the Swiss National Science Foundation (SNSF).

References

[1] Ji Y, Chung Y, Sprinzak D, Heiblum M, Mahalu D and Shtrikman H 2003 *Nature* **422** 415–8
[2] Hasselbach F 2010 *Rep. Prog. Phys.* **73** 016101
[3] Rauch H and Werner S A 2000 *Neutron Interferometry: Lessons in Experimental Quantum Mechanics* (Oxford: Oxford University Press)
[4] Cronin A D, Schmiedmayer J and Pritchard D E 2009 *Rev. Mod. Phys.* **81** 1051–129
[5] de Broglie L 1923 *Nature* **112** 540
[6] Hornberger K, Gerlich S, Ulbricht H, Hackermüller L, Nimmrichter S, Goldt I, Boltalina O and Arndt M 2009 *New J. Phys.* **11** 043032
[7] Berninger M, Stefanov A, Deachapunya S and Arndt M 2007 *Phys. Rev.* A **76** 013607
[8] Schöllkopf W and Toennies J P 1994 *Science* **266** 1345–8
[9] Buyvol-Kot F, Kalinin A, Kornilov O, Toennies J and Becker J 2005 *Solid State Commun.* **135** 532–7
[10] Bonin K D and Kresin V V 1997 *Electric-Dipole Polarizabilities of Atoms, Molecules and Clusters* (Singapore: World Scientific) ISBN 981-02-2493-1
[11] Tüxen J, Gerlich S, Eibenberger S, Arndt M and Mayor M 2010 *Chem. Commun.* **46** 4145–7
[12] Ulbricht H, Berninger M, Deachapunya S, Stefanov A and Arndt M 2008 *Nanotechnology* **19** 045502
[13] Gerlich S, Gring M, Ulbricht H, Hornberger K, Tüxen J, Mayor M and Arndt M 2008 *Angew. Chem., Int. Ed. Engl.* **47** 6195–8
[14] Nimmrichter S and Hornberger K 2008 *Phys. Rev.* A **78** 023612
[15] Gring M *et al* 2010 *Phys. Rev.* A **81** 031604
[16] Gerlich S *et al* 2007 *Nat. Phys.* **3** 711–5
[17] Knight W D, Clemenger K, de Heer W A and Saunders W A 1985 *Phys. Rev.* B **31** 2539–40
[18] de Heer W A 1993 *Rev. Mod. Phys.* **65** 611–76
[19] Antoine R, Rayane D, Allouche A R, Aubert-Frécon M, Benichou E, Dalby F W, Dugourd P and Broyer M 1999 *J. Chem. Phys.* **110** 5568–77
[20] de Heer W A and Kresin V V 2010 Electric and magnetic dipole moments of free nanoclusters *Handbook of Nanophysics* ed K D Sattler (Boca Raton, FL: CRC Press)
[21] Compagnon I, Antoine R, Rayane D, Dugourd P and Broyer M 2001 *Eur. Phys. J.* D **16** 365–8
[22] Broyer M, Antoine R, Compagnon I, Rayane D and Dugourd P 2007 *Phys. Scr.* C **76** 135
[23] Filsinger F, Erlekam U, von Helden G, Küpper J and Meijer G 2008 *Phys. Rev. Lett.* **100** 133003(4)
[24] Arndt M, Nairz O, Petschinka J and Zeilinger A 2001 *C. R. Acad. Sci. Paris* **2, Série IV** 581–5
[25] Brezger B, Arndt M and Zeilinger A 2003 *J. Opt. B: Quantum Semiclass. Opt.* **5** S82–9
[26] Compagnon I, Antoine R, Rayane D, Broyer M and Dugourd P 2002 *Phys. Rev. Lett.* **89** 253001(4)
[27] Zimmermann T J and Müller T J J 2002 *Synthesis* **9** 1157–62
[28] Rathore R, Burns C L and Guzei I A 2004 *J. Org. Chem.* **69** 1524–130
[29] Burkert U and Allinger N L 1984 *Molecular Mechanics* (Washington, DC: American Chemical Society)
[30] Stefanov A, Berninger M and Arndt M 2008 *Meas. Sci. Technol.* **19** 055801
[31] Van Vleck J 1932 *The Theory of Electric and Magnetic Susceptibilities* (London: Oxford University Press)
[32] Frisch M J *et al* 2009 *Gaussian 09 Revision A.02* (Wallingford, CT: Gaussian Inc.)
[33] Deachapunya S, Stefanov A, Berninger M, Ulbricht H, Reiger E, Doltsinis N L and Arndt M 2007 *J. Chem. Phys.* **126** 164304
[34] Huszánk R and Horváth O 2005 *Chem. Commun.* **2** 224–6
[35] Ghosh A 2000 Quantum chemical studies of molecular structures and potential energy surfaces of porphyrins and hemes *The Porphyrin Handbook* vol 7, ed K M Kadish *et al* (New York: Academic) pp 1–38